Supporting Information

Synergistic engineering of bromine and ctyltrimethylammonium chloride molecule enabling efficient and stable flexible perovskite solar cells

Hao Mei[a,b,†], Yuliang Wu[c,†], Changlei Wang[a,b,*], Shengqiang Ren[d], Mingdi Zhang[e], Haitao Dai[e], Dewei Zhao[d], Zhengying Li[c], Qingguo Du[c,*] and Xiaofeng Li[a,b,*]

[a]*School of Optoelectronic Science and Engineering & Collaborative Innovation Center of Suzhou Nano Science and Technology, Soochow University, Suzhou 215006, China.*

[b]*Key Lab of Advanced Optical Manufacturing Technologies of Jiangsu Province & Key Lab of Modern Optical Technologies of Education Ministry of China, Soochow University, Suzhou 215006, China.*

[c]*School of Information Engineering, Wuhan University of Technology, 122 Luoshi Road, Wuhan, Hubei 430070, China.*

[d]*Institute of Solar Energy Materials and Devices, College of Materials Science and Engineering, Sichuan University, No. 24 SouthSection 1, Yihuan Road, Chengdu 610064, China.*

[e]*School of Precision Instrument & Optoelectronics Engineering, Tianjin University, Tianjin 300072, China.*

†These authors contributed equally to this work.

**Corresponding authors: cl.wang@suda.edu.cn;qingguo.du@whut.edu.cn; xfli@suda.edu.cn.*

Experimental Section

1.Preparation of SnO_2 layers

SnO_2 aqueous solution (15%) was purchased from Alfa Aesar. SnO_2 layer was spin-coated on a flexible PET substrate. Prior to spin coating, the substrate was washed with UV light for 30minutes. The SnO_2 stock solution and deionized water were mixed at a volume ratio of 1:5, spin-coated at 500 rpm for 3 seconds, 4000 rpm for 30 seconds, and then heated at 105℃ for 20 mins to complete the preparation of SnO_2 electron transport layers.

2. Preparation of perovskite precursors

The $MA_{0.7}FA_{0.3}PbI_3$perovskite precursor solution was prepared by adding methyl ammonium iodide (MAI, 99.9%, Advanced Election Technology Co.,Ltd), formamidine iodide (FAI, 99.9%, Xi'an Polymer Light Technology Corp.), lead iodide (PbI_2, 99.99%, Xi'an Polymer Light Technology Corp.) and lead thioycanate ($Pb(SCN)_2$, 98.5%, Sigma Aldrich) with a molar ratio of 0.7:0.3:1:0.03 in dimethyl sulfoxide (DMSO, 99.8%, Sigma Aldrich) and N, N-dimethylformamide (DMF, 99.8%, Sigma Aldrich) mixture with volume ratio of 1:9. $MA_{0.7}FA_{0.3}Pb(I_{1-x}Br_x)_3$ perovskite precursors were prepared by mixing $MA_{0.7}FA_{0.3}PbI_3$ and $MA_{0.7}FA_{0.3}Pb(I_{0.9}Br_{0.1})_3$ with different volume ratios. Prior to spin coating, the solutions were heated to 60℃ overnight for sufficient dissolving and the purified with 0.45 μm filters.

3. Fabrication of flexible PVSCs

The whole processes were carried out in a nitrogen-filled glove box. The perovskite precursor solution was spin-coated on electron transporting layer at 500 rpm for 3 seconds, 4000 rpm for 60 seconds. And then chlorobenzene (CB, 99%, Sigma Aldrich) was used as an anti-solvent at 7s of the second stage. 0.08% CTAC was dissolved in CB under stirring for 12 hours. After dilution with CB, 0.005%, 0.01%, 0.02%, and 0.04% CTAC solutions were obtained, which were then dropped on the surface of perovskite films as anti-solvents. After that, the perovskite film was heated at 65 ℃ for 2 minutes and 100 ℃ for 5 minutes. We use 2,2',7,7'-tetrakis(N,N'-di-*p*-methoxyphenylamine)-9,9'-spirobifluorene (Spiro-OMeTAD) as hole transporting layer and spin coated on the perovskite film with 500 rpm for 3 seconds, 4500 rpm for 40 seconds. The Spiro-OMeTAD solution was prepared by dissolving 72.3 mg of Spiro-OMeTAD (99.0%) in 1 mL of CB, adding 28 μL of tetra-tert-butylpyridine (TBP) (Xi'an Polymer), and 18 μL Li-bis (trifluoromethanesulfonyl)

imide (Li-TFSI) (Xi'an Polymer, 99.95%) (520 mg/mL in acetonitrile) and 18 μL Co(II)-TFSI salt (FK209, Xi'an Polymer) (300 mg/mL in acetonitrile). The electrode deposited a layer of 70 nm silver (Ag) on the top of Spiro-OMeTAD by thermal evaporation and the working area of the device defined by the mask to be 0.07 cm^2. For large area flexible devices, metal mask with area of 1 cm^2 was used to define the working area. For the stability test, we fabricated large amount of sub-cells and then put them under high humidity for different times. The films were taken out and put into inert atmosphere until all of the films are ready. The sub-cells are perovskite films deposited on SnO_2 ETLs, without spin-coating of Spiro-OMeTAD and metal layers. It was found that Spiro-OMeTAD would be disabled upon high humidity exposure; therefore, in order to get rid of the effect of Spiro-OMeTAD layer on the final performance, we just test the influence of perovskite layer with moisture. When all of the sub-cells were taken out, we spin-coated Spiro-OMeTAD layer and evaporated metal layer for all. Then we measured the photovoltaic performance of flexible PVSCs. This way do not obey the International Summit on Organic Photovoltaic Stability (ISOS) protocols, since we care more about the stability of perovskite film against moisture influence excluding the affection of Spiro-OMeTAD and other materials.

4. Characterizations

A solar simulator (Newport) was used as the light source to measure the *J-V* curve with alight intensity of 100 mW/cm^2, and a Keithley 2400 sourcemeter was used to record the data. EQE measurements were performed using the EQE system and other near-dark test conditions using 100 Hz chopped monochromatic light from 280 nm to 900 nm. Field emission SEM instrument (Hitachi S-4800) was used to characterize the top view and cross-sectional structure of the perovskite films and PVSCs. For steady-state photoluminescence (PL) and time-resolved photoluminescence (TRPL) measurements, perovskite films were prepared by spin-coating perovskite precursors on SLG glass substrates and then coated with another polymethyl methacrylate (PMMA) layer. Water contact angle was conducted using DSA100. The XRD pattern was scanned from 5° to 60° at a rate of 5° per minute using a Bruker D8 advance diffractometer model. The transmission and absorbance spectrum of the perovskite layer was measured using the UV-3600PC ultraviolet-visible-near infrared (UV-vis-NIR) spectrometer with a glass layer as the baseline. The scan rate is medium speed and the range is 300-1000nm.

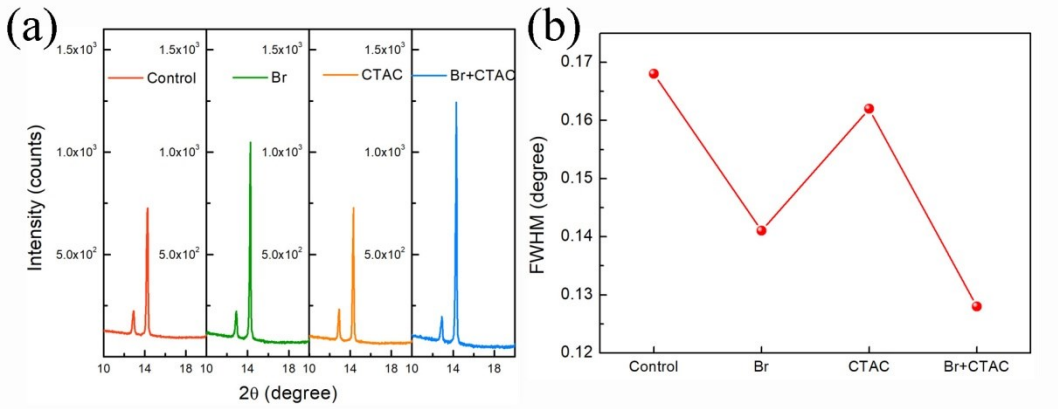

Figure S1. (a) XRD patterns (10-19 degree) and (b) FWHM of (110) peak of perovskite films with different treatments.

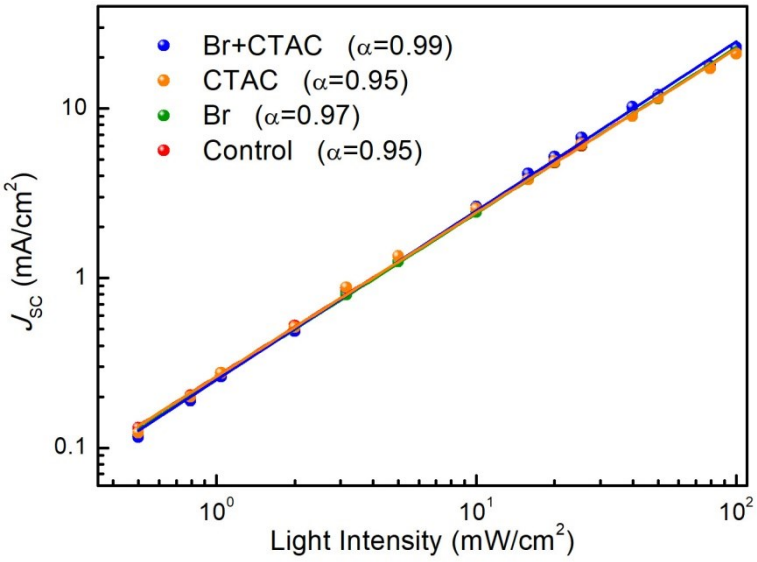

Figure S2. Light intensity of J_{SC} of perovskite devices with different treatments. The power law dependence of J_{SC} on the light intensity shows a linear relation in a double logarithmic scale. The fitted slopes (α) of these PVSCs are 0.99, 0.95 and 0.97 and 0.95 for Br+CTAC, CTAC, Br, and Control, respectively. It has been reported that a solar cell with no space charge limited photocurrents will give a slope of 1. The PVSC with Br and Br+CTAC has more balanced charge carrier transportation than the control and CTAC PVSCs due to the improved perovskite film quality.

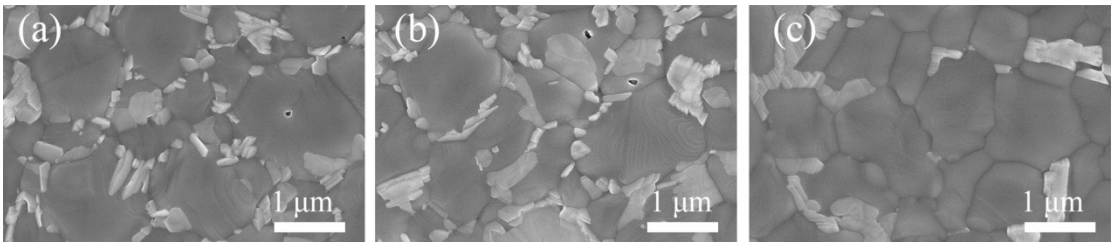

Figure S3. SEM images of perovskite films with (a) 2.5%, (b) 7.5% and (c) 10% Br. The scale bar is 1 μm for all.

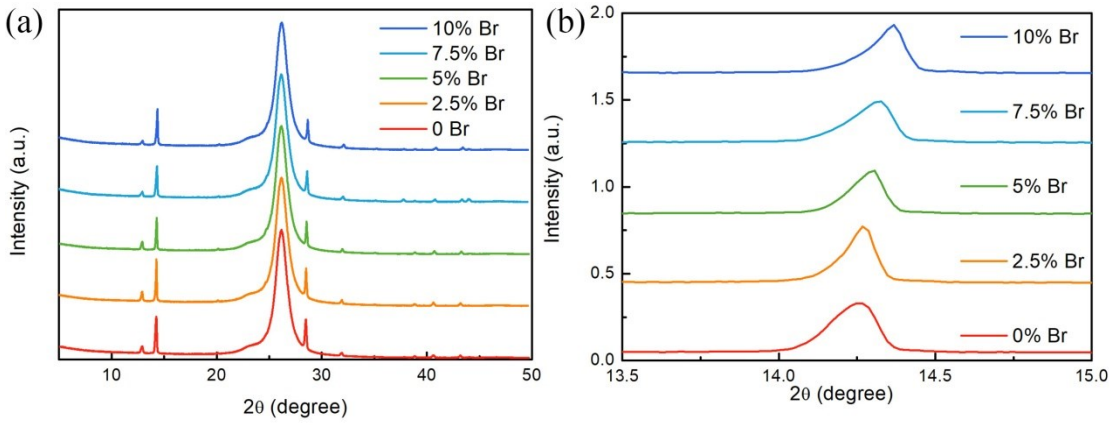

Figure S4. XRD patterns of perovskite films with different concentrations of Br.

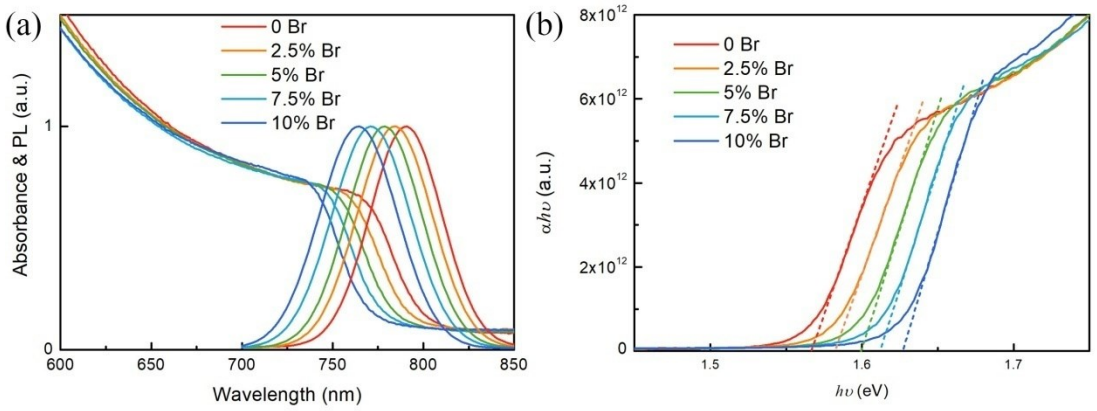

Figure S5. Tauc-plots of perovskite films with different concentrations of Br.

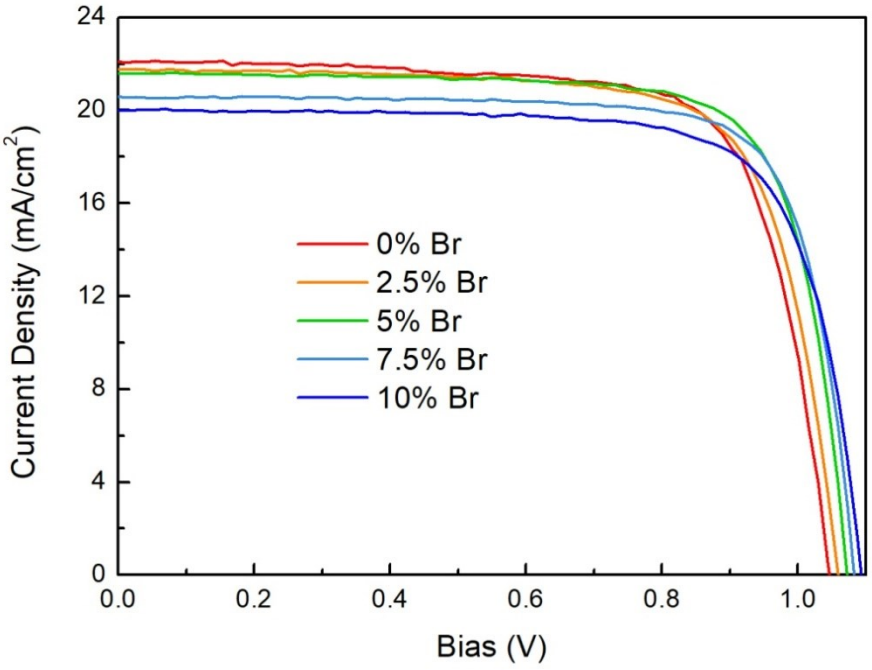

Figure S6. *J-V* curves of flexible PVSCs containing various amounts of Br.

Table S1. The photoelectric properties of *J-V* curves shown in **Figure S4**.

Br Concentration	**PCE (%)**	**V_{OC} (V)**	**J_{SC} (mA/cm^2)**	**FF**
0%	17.04	1.047	22.08	0.737
2.5%	17.05	1.059	21.76	0.741
5%	17.51	1.072	21.61	0.756
7.5%	16.69	1.083	20.59	0.749
10%	16.43	1.093	20.02	0.751

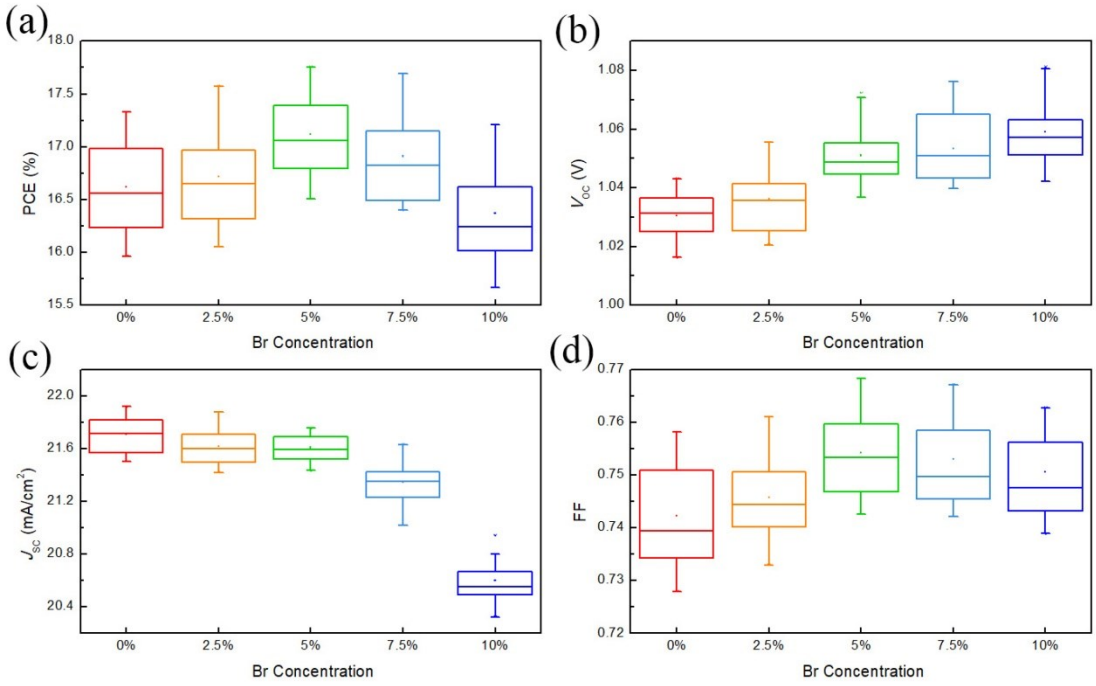

Figure S7. Statistical results of (a) PCE, (b) V_{OC}, (c) J_{SC} and (d) FF of flexible PVSCs with different amounts of Br.

Table S2. The photoelectric properties of PVSCs with different concentrations of Br. The results were calculated with 20 devices. The error values represent standard deviations.

Br Concentration	**PCE (%)**	**V_{OC} (V)**	**J_{SC} (mA/cm^2)**	**FF**
0%	16.61±0.42	1.030±0.008	21.71±0.13	0.742±0.009
2.5%	16.72±0.43	1.036±0.010	21.62±0.14	0.746±0.007
5%	17.11±0.38	1.051±0.009	21.61±0.09	0.754±0.008
7.5%	16.91±0.43	1.053±0.011	21.35±0.15	0.753±0.008
10%	16.37±0.46	1.059±0.011	20.60±0.17	0.750±0.008

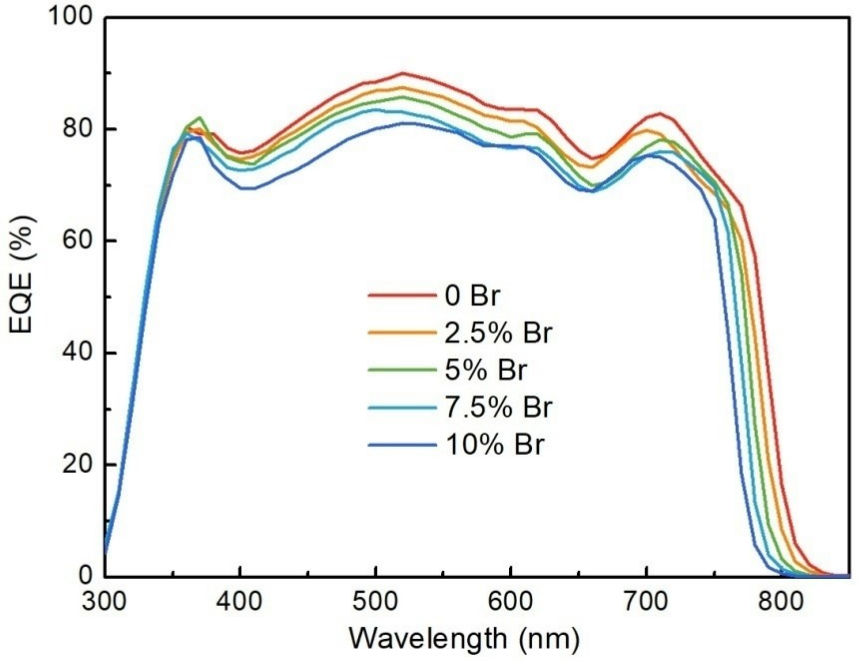

Figure S8. EQE of PVSCs containing various amounts of Br.

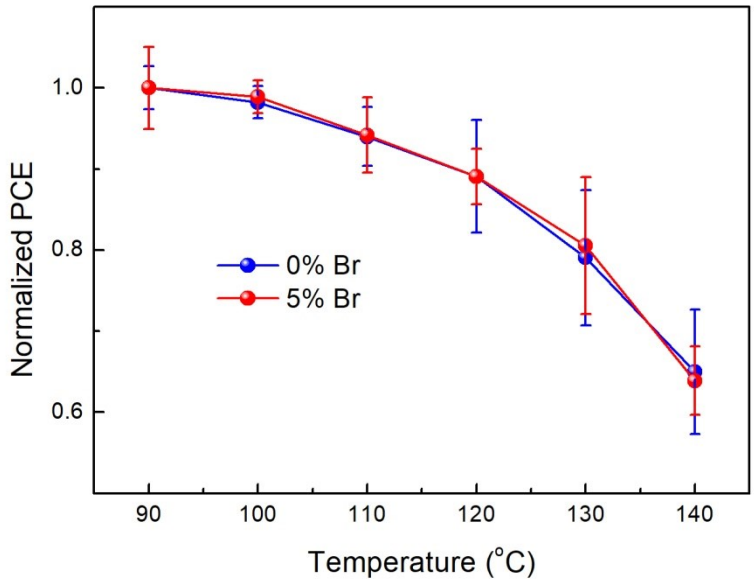

Figure S9. Thermal stability of PVSCs fabricated from sub-cells with 0% and 5% Br. The sub-cells are perovskite films coated on ETL on rigid FTO/glass substrates, and then been annealed at different temperatures from 90 to 140 °C for 1 hour at each temperature. After thermal stresses, these sub-cells are collected and then finished with HTL/Ag back contacts for performance characterizations.

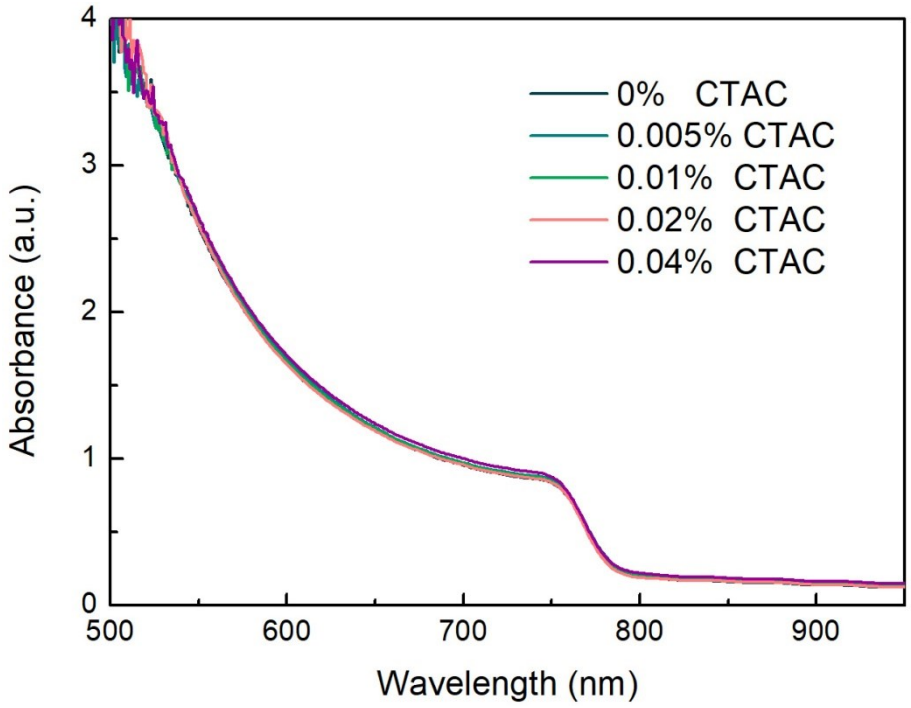

Figure S10. Absorbance spectra of perovskite films containing various amounts of CTAC.

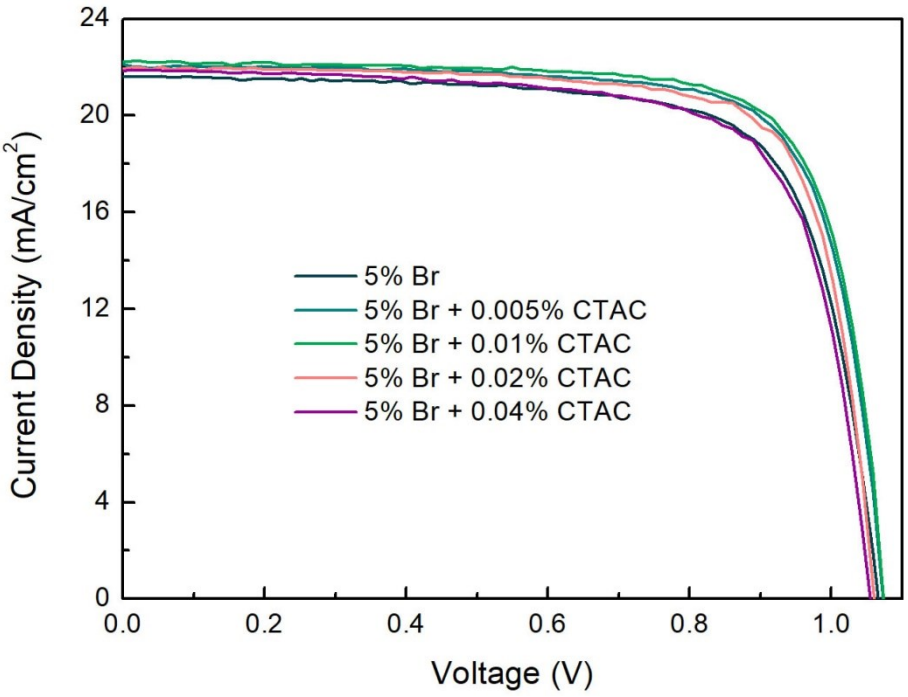

Figure S11. *J-V* curves of flexible PVSCs containing various amounts of CTAC.

Table S3. Photovoltaic performance of flexible PVSCs with different weight ratios of CTAC.

CTAC weight ratio	**PCE (%)**	**V_{OC} (V)**	**J_{SC} (mA/cm^2)**	**FF**
0%	17.51	1.072	21.61	0.756
0.005%	17.96	1.073	22.12	0.757
0.01%	18.20	1.075	22.18	0.763
0.02%	17.73	1.065	21.95	0.758
0.04%	16.89	1.054	21.85	0.733

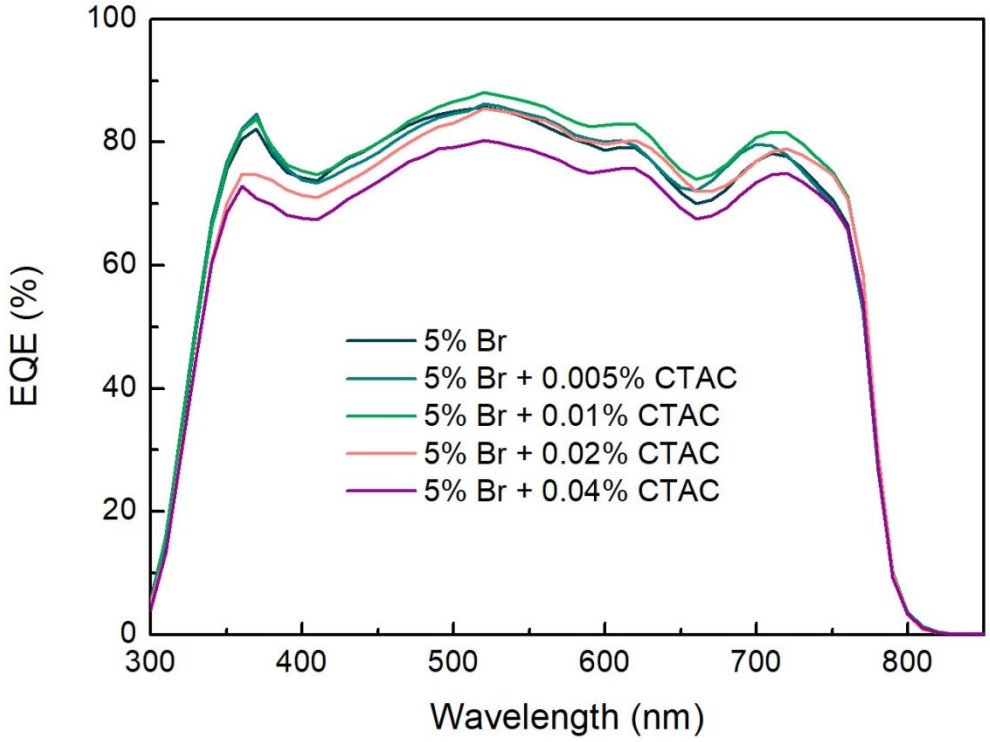

Figure S12. EQE of PVSCs containing various amounts of CTAC.

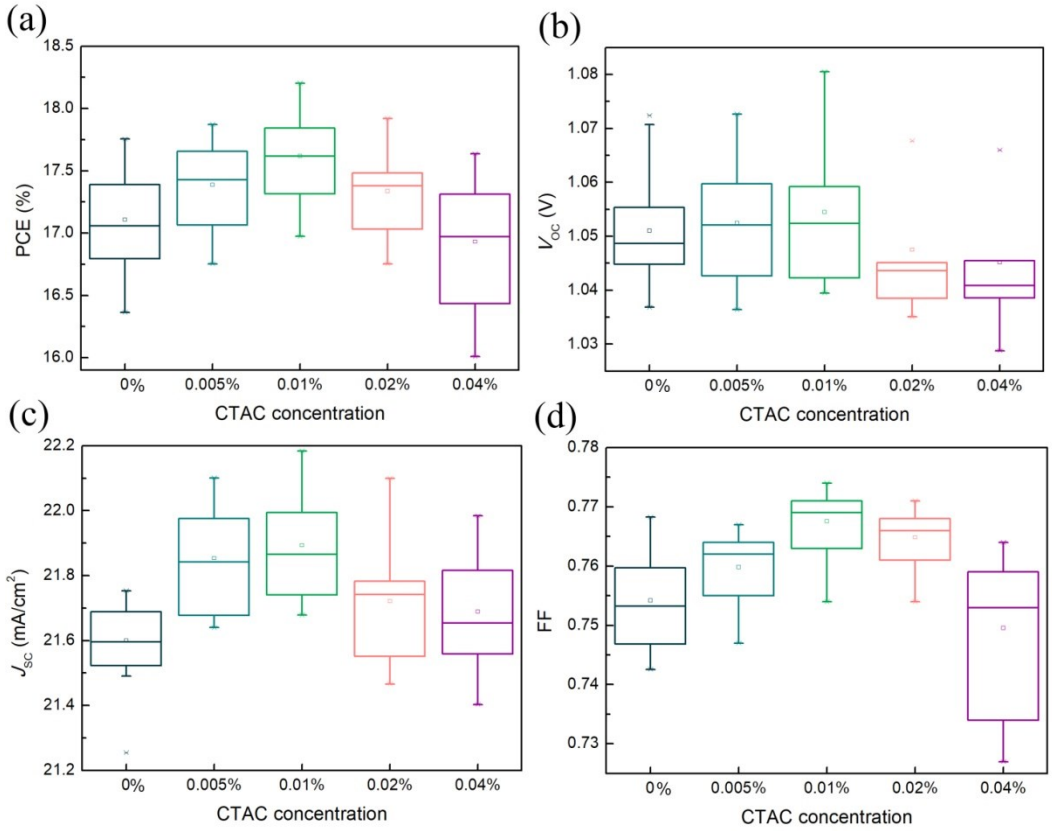

Figure S13. Statistical results of (a) PCE, (b) V_{OC}, (c) J_{SC} and (d) FF of flexible PVSCs with different amounts of CTAC.

Table S4. The photoelectric properties of PVSCs with different concentrations of CTAC. The results were calculated with 20 devices. The error values represent standard deviations.

CTAC Concentration	**PCE (%)**	**V_{OC} (V)**	**J_{SC} (mA/cm^2)**	**FF**
0%	17.10±0.40	1.051±0.009	21.60±0.12	0.754±0.008
2.5%	17.38±0.37	1.052±0.011	21.85±0.16	0.760±0.007
5%	17.61±0.34	1.055±0.012	21.89±0.15	0.768±0.006
7.5%	17.33±0.33	1.047±0.011	21.72±0.19	0.765±0.005
10%	16.93±0.50	1.045±0.012	20.69±0.17	0.750±0.012

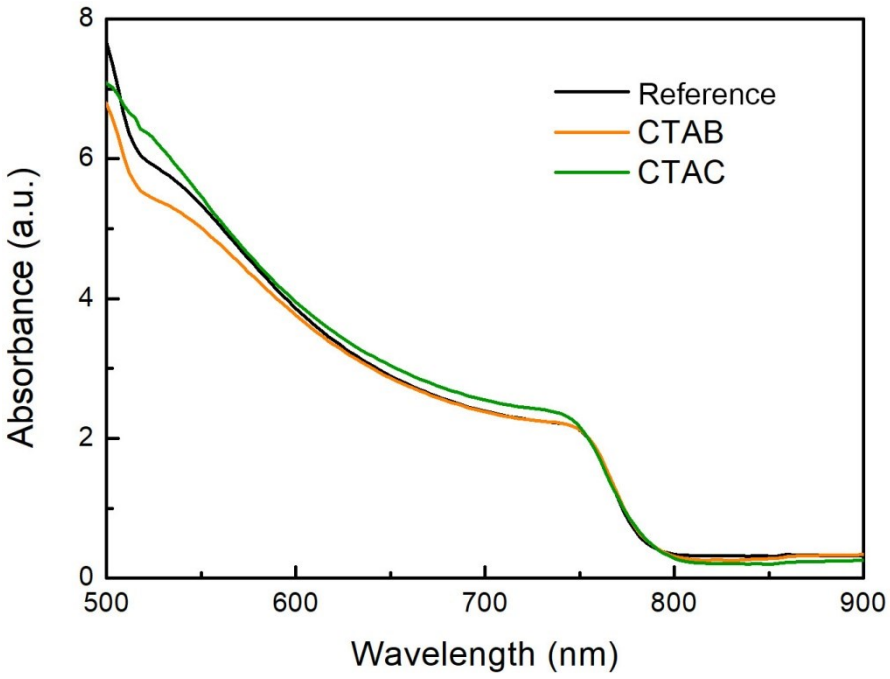

Figure S14. Absorbance spectra of perovskite films with no coating (control), and with CTAB and CTAC surface treatments.

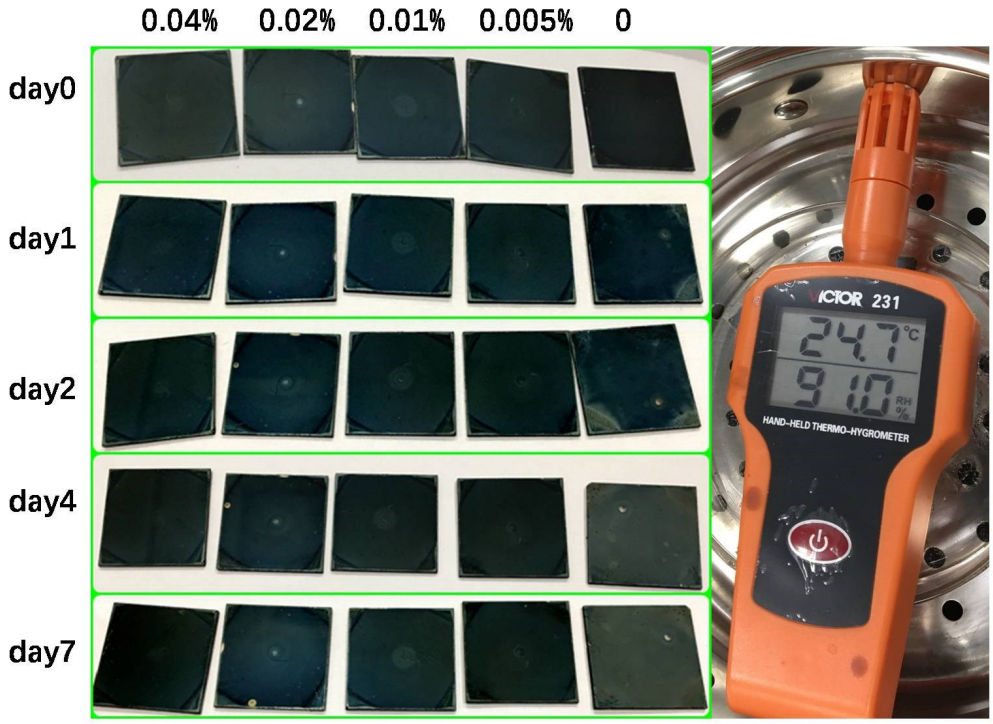

Figure S15. Stability test of perovskite films containing different contents of CTAC exposed to 90% high humidity.

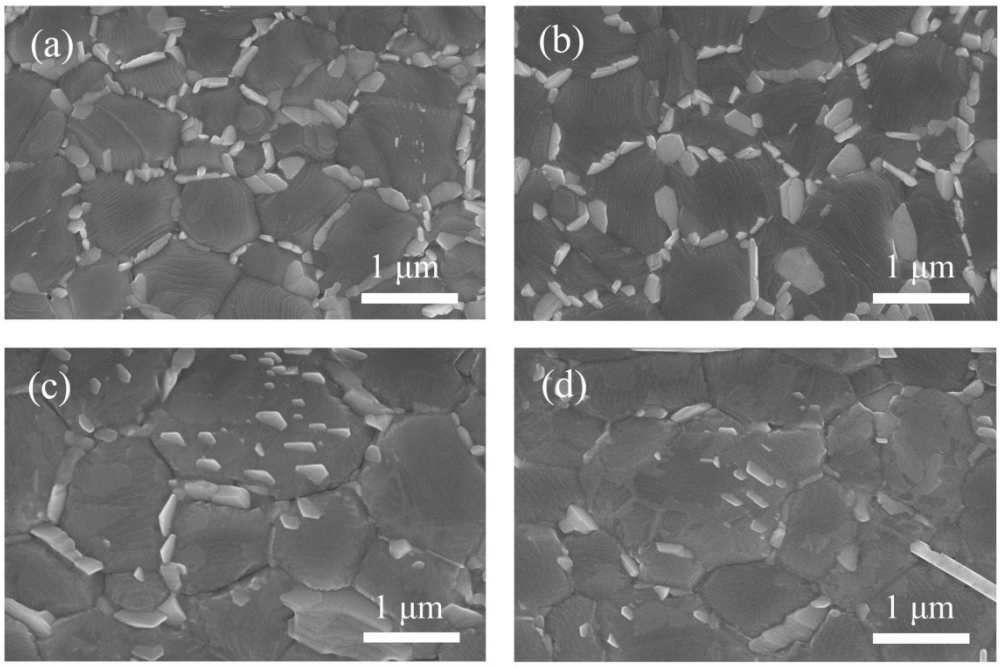

Figure S16. SEM morphology of control perovskite film (a) before and (b) after 200 times bending; SEM images of CTAC coated perovskite film (c) before and (d) after 200 times bending.